



Immune-phenotyping of pleomorphic dermal sarcomas suggests this entity as a potential candidate for immunotherapy

Sebastian Klein^{1,3} · Cornelia Mauch² · Svenja Wagener-Rydzek³ · Maximilian Schoemmel³ · Reinhard Buettner³ · Alexander Quaas³ · Doris Helbig²

Received: 1 November 2018 / Accepted: 3 April 2019 / Published online: 8 April 2019
© Springer-Verlag GmbH Germany, part of Springer Nature 2019

Abstract

Background Pleomorphic dermal sarcomas (PDS) are sarcomas of the skin with local recurrences in up to 28% of cases, and distant metastases in up to 20%. Although recent evidence provides a strong rationale to explore immunotherapeutics in solid tumors, nothing is known about the immune environment of PDS.

Methods In the current study, a comprehensive immune-phenotyping of 14 PDS using RNA and protein expression analyses, as well as quantitative assessment of immune cells using an image-analysis tool was performed.

Results Three out of 14 PDS revealed high levels of CD8-positive tumor-infiltrating T-lymphocytes (TILs), also showing elevated levels of immune-related cytokines such as IL1A, IL2, as well as markers that were very recently linked to enhanced response of immunotherapy in malignant melanoma, including CD27, and CD40L. Using a multivariate analysis, we found a number of differentially expressed genes in the CD8-high group including: *CD74*, *LYZ* and *HLA-B*, while the remaining cases revealed enhanced levels of immune-suppressive cytokines including *CXCL14*. The “CD8-high” PDS showed strong MHC-I expression and revealed infiltration by PD-L1-, PD-1- and LAG-3-expressing immune cells. Tumor-associated macrophages (TAMs) predominantly consisted of CD68+, CD163+, and CD204+ M2 macrophages showing an accentuation at the tumor invasion front.

Conclusions Together, we provide first explorative evidence about the immune-environment of PDS tumors that may guide future decisions whether individuals presenting with advanced PDS could qualify for immunotherapeutic options.

Keywords Immune-phenotyping · Major histocompatibility complex (MHC) · NanoString · Pleomorphic dermal sarcoma (PDS) · RNA analysis · Tumor-infiltrating lymphocytes (TILs)

Abbreviations

CPI Immune checkpoint inhibitors
FFPE Formalin-fixated and paraffin-embedded

M1 Type 1 macrophages
M2 Type 2 macrophages
PDCD1 Programmed cell death 1
PDS Pleomorphic dermal sarcoma
TAM Tumor-associated macrophages
TIGIT T cell immunoreceptor with Ig and ITIM domains
TMA Tissue microarray

Alexander Quaas and Doris Helbig contributed equally.

Electronic supplementary material The online version of this article (<https://doi.org/10.1007/s00262-019-02339-3>) contains supplementary material, which is available to authorized users.

✉ Doris Helbig
doris.helbig@uk-koeln.de

¹ Else Kröner Forschungskolleg Clonal Evolution in Cancer, University Hospital Cologne, Weyertal 115b, 50931 Cologne, Germany

² Department of Dermatology, University Hospital Cologne, Kerpener Strasse 62, 50937 Cologne, Germany

³ Institute of Pathology, University Hospital Cologne, Cologne, Germany

Introduction

Pleomorphic dermal sarcomas (PDS) are cutaneous sarcomas developing in UV-dependent locations. Although the exact prevalence remains unknown, PDS are considered frequent within the group of cutaneous sarcomas. Clinically, these tumors can be treated by curative excisions, although local recurrences occur in up to 28% of cases, and distant

metastases have been described in up to 20% of these individuals, respectively [1, 2]. In addition, characteristic UV-induced *TP53* mutations can be found in almost all cases of PDS, and about one-third of PDS harbor activating *PIK3CA* or *RAS* mutations, as well as *ALK* translocations, and thus reveal potentially targetable genetic alterations [3, 4].

Recent advances have allowed to reprogram immune cells using molecules that target mechanisms of T cell exhaustion, including anti-PD-1/PD-L1, as well as anti-(CTLA)-4 [5]. Until now, only a limited number of biomarkers have been clinically established to predict response to immunotherapy, including PD-L1, and very recently tumor mutation burden [6–10]. In addition, the surrounding tumor environment of immune cells, blood vessels, as well as stromal cells generates a distinct milieu that influences response to therapy in general, but given the nature of the mechanism of action, to a larger extent to immune checkpoint inhibitors (CPI) [11, 12]. In this context, gene expression profiles of the tumor cells, as well as the composition of TILs, tumor-suppressing M1 and tumor-promoting M2 macrophages may help to understand the immunological phenotype of a given tumor [13–15].

In different other tumor entities, treatment response to PD-1/PD-L1 or cytotoxic T-lymphocyte-associated protein (CTLA)-4 pathway blockade correlated with the amount of tumor-infiltrating CD8+ T cells, PD-L1 as well as MHC class I expression [16–19]. Together, nothing is known about the immune environment of PDS, and there is a need to uncover potential vulnerabilities towards therapeutic approaches on the basis of immune-modulation for patients presenting with advanced stages of PDS.

Therefore, the aim of the current study was to give a comprehensive immune-phenotyping of PDS tumors using RNA expression analyses, as well as quantitative assessment of immune cells, in addition to markers of immune response, including MHC class I/II.

Materials and methods

Patient characteristics and tumor material

We analyzed formalin-fixated and paraffin-embedded (FFPE) material of 14 patients with PDS who underwent primary surgical resection at the Department of Dermatology, University of Cologne, Germany between 2010 and 2017. All tumors were re-evaluated by Doris Helbig and Alexander Quaas according to our definition, following the introduction of the term by Fletcher [20]; PDS are predominant dermal tumors composed of atypical and proliferating pleomorphic and spindle cells infiltrating into deeper structures, such as the subcutaneous fat or muscles. All investigated tumors developed in elderly patients (> 58 years old) and were located in UV-exposed skin locations (see Table 1).

Table 1 Patient and tumor characteristics

	PDS (<i>n</i> = 14)
Male	11
Female	3
Age (years)	
– Range	58–92
– Median	75.5
– Mean	76
Tumor location	
– Head/Neck	12
– Shoulder	2

Macrodissection and RNA isolation

Ten-micrometer thin sections were cut from FFPE tissue blocks for RNA extraction. Six sections of 10 µm thickness were deparaffinized and the tumor areas were macrodissected from unstained slides using a marked hematoxylin–eosin (H&E)-stained slide as a reference. For extraction purpose, the Maxwell RSC RNA FFPE Kit was used on the Maxwell RSC (Promega) according to manufacturer's instruction, including DNase digestion. Quantification of RNA was done using a NanoDrop spectrophotometer.

RNA expression profiles using NanoString

Differential expression of immune-related genes on mRNA level was determined using the NanoString PanCancer IO360 Profiling Panel (NanoString Technologies, Inc., Seattle, WA). Isolated RNA was hybridized to a set of 770 specific and fluorescently labeled gene probes for 18 h at 65 °C. Afterwards, hybridization products were prepared for cartridge loading on an nCounter PrepStation. Digital Counting of fluorescent signals was conducted using the nCounter Digital Analyzer. Forty housekeeping genes were used for normalization purpose with help of the nsolver3.0 software. Subsequent statistical analyses were done using *R*, the *R*-Project.

Immunohistochemistry (IHC)

Immunohistochemical staining was performed on full tumor sections using the BOND MAX from Leica (Leica, Germany) according to the protocol of the manufacturers. For details of all antibodies see Table 2.

For the purpose of quantifying CD3, CD8 and CD20-positive lymphocytes, slides were scanned using a NanoZoomer S360 (Hamamatsu Photonics) slide scanner. Subsequently, the analysis was performed using QuPath (v0.1.2 [21]). Tumor areas were defined as region-of-interest and

Table 2 Antibodies used for immunohistochemistry

Antibody specificity	Species and type	Clone	Source	Conditions
CD3	Rabbit; IgG	SP7	Thermo	Citrate; 1:50
CD8	Mouse; IgG1	CD8	Dako	Citrate; 1:200
CD20	Mouse; IgG2a	L26	Dako	Citrate; 1:1250
CD68	Mouse; IgG3	PG-M1	Dako	EDTA; 1:400
CD163	Mouse; IgG1	MRQ-26	Cellmarque	EDTA; 1:100
CD204	Mouse; IgG1	SRA-E5	Abnova	EDTA; 1:200
LAG-3	Rabbit; IgG	D2G40	Cell signaling	EDTA; 1:300
MHC-I	Rabbit	EPR1394y	Abcam	Citrate; 1:300
MHC-II	Rabbit	EPR 11,226	Abcam	EDTA; 1:3000
PD-L1	Rabbit; IgG	28–8	Abcam/Dako	EDTA; 1:100
PD-1	Mouse; IgG1	ab5	Abcam	EDTA; 1:200

divided into three parts: tumor apical (close to the surface), tumor center and tumor basal (infiltration margins into the surrounding soft tissue), while the whole-area was defined as all areas together. All quantitative measurements were normalized to the total amount of cells being counted. After quantification of all cases for CD8-positive TILs, cases were categorized into PDS with an elevated immune cell infiltration and cases with almost no detectable CD8-positive T cells. In the group of PDS with an elevated immune cell infiltration, those cases with CD8 levels above median were marked as “CD8-high”, all other cases as “CD8-low”.

All other immunostainings were scored manually by one dermatopathologist (Doris Helbig) and one pathologist (Alexander Quaas) independently as follows (see further description for quantification).

MHC class I and II expression by tumor cells

MHC class I tumor cell membrane staining was scored using the Allred method [22]: a score between 0 and 8 is determined from the sum of a membrane proportion score reflecting the fraction of cells with any stain (0 = 0%; 1 < 1%; 2 = 1–10%; 3 = 11–33%; 4 = 34–66%; 5 = 67–100% cells stained), and a membrane intensity score reflecting the strength of staining among the positive cells (0 = not reactive; 1 = weakly reactive; 2 = moderately reactive; 3 = strongly reactive).

MHC class II expression was classified as positive (score = 1) if a cutoff of > 5% of tumor cells showed a membranous staining in accordance to Johnson et al. [23].

Expression of PD-L1, PD-1 and LAG-3 on tumor and/or inflammatory cells

The proportions of membrane-bound PD-L1-positive cells were scored as described by Scheel et al. as “Consensus Score” (0: < 1%; 1: $\geq 1 < 5\%$; 2: $\geq 5 < 10\%$; 3: $\geq 10 < 25\%$; 4: $\geq 25 < 50\%$; 5: $\geq 50\%$) [24]. A tumor cell was considered

PD-L1 positive if the cell membrane was partially or completely stained whereas cytoplasmic PD-L1 staining was considered negative [25]. Moreover, the ratio of stained and unstained cells (number of PD-L1 + tumor cells divided by the number of all tumor cells) was evaluated [25]. Immune cells such as macrophages and lymphocytes were considered “PD-L1 positive” if a membranous and/or cytoplasmic staining was seen and quantified by evaluating the ratio of the area covered by stained immune cells (area covered by PD-L1 + immune cells ÷ tumor area) [26]. A case was considered as “positive” if $\geq 1\%$ of the respective cells showed a specific staining of any intensity.

For quantification of PD-1 expression on inflammatory cells, we defined a cutoff of 1%. The following scoring system for PD-1 was used: 0: < 1%, 1: $\geq 1–2\%$, 2: $\geq 2–5\%$ and 3: > 5% of all TILs.

Due to the experiences made with PD-L1 in the past, we defined a cutoff of at least 1% LAG-3-expressing inflammatory cells to define a tumor as LAG-3 positive. LAG-3-positive inflammatory cells were rated in relation to all TILs. The amount of LAG-3-positive inflammatory cells was scored as 0: < 1%, 1: $\geq 1–2\%$, 2: $\geq 2–5\%$ and 3: > 5% of all TILs.

Tumor-associated macrophages

The infiltration of CD68-positive, CD163-positive and CD204-positive macrophages was graded semi-quantitatively in concern of the tumor center and the invasive front (tumor apical and tumor basal) in accordance to Jensen et al. [27]. Briefly, macrophage infiltration of the tumor was graded from 0 (none or rare infiltrating cells) to 4 (massive infiltration of macrophages).

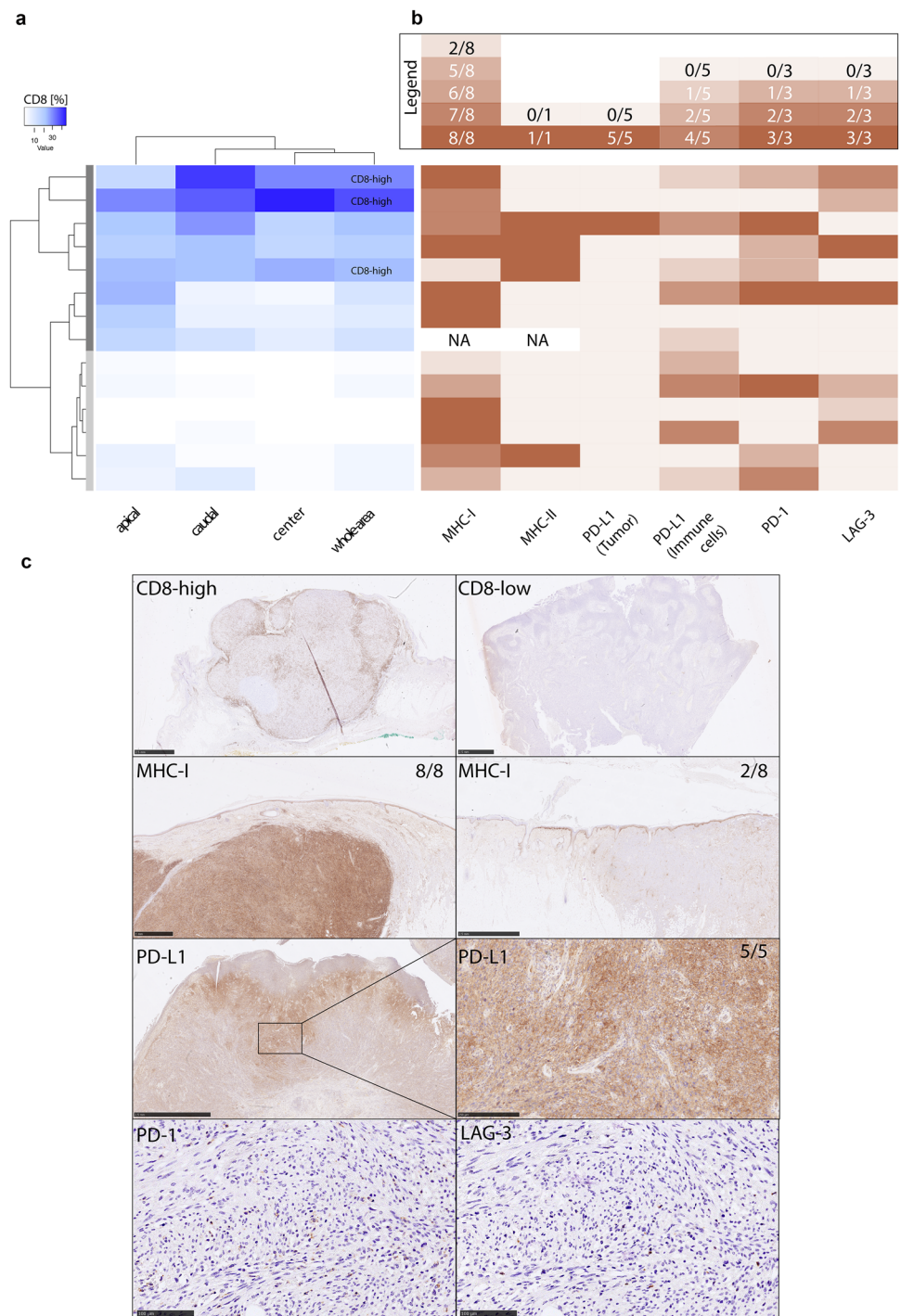
Results

Quantification of CD3, CD8 and CD20-positive immune cell infiltration

Out of 14 PDS investigated for CD8-positive TILs using an image-analysis tool, 8 cases presented with an

elevated immune cell infiltration, while 6 cases revealed a phenotype with almost no detectable CD8-positive T cells. The median value of CD8-positive cells was 9.8% for the whole tumor area. Three cases with CD8 levels above median were marked as “CD8-high” (see Fig. 1a). The differences of CD8-positive TILs within the infiltration margins (apical and basal) compared to the center of the tumor did not reach statistical significant difference,

Fig. 1 Exploring the immune microenvironment in PDS. **a** Quantitative analysis of CD8 positive immune cells using an image-analysis tool reveals eight cases (dark grey bar) out of 14 cases showing an elevated immune cell infiltration, while six cases (light grey bar) revealed a phenotype with almost no detectable CD8 positive T cells. Three cases with CD8 levels above median were marked as “CD8-high”. **b** Quantitative analysis of various markers including MHC-I (score 0–8 using the Allred method), MHC-II (score 0–1 with a cutoff of > 5% of tumor cells show a membranous staining in accordance to Johnson), PD-L1 on tumor, as all as PD-L1 and LAG-3 on immune cells [“Consensus Score” by Scheel et al. (0: < 1%; 1: ≥ 1 < 5%; 2: ≥ 5 < 10%; 3: ≥ 10 < 25%; 4: ≥ 25 < 50%; 5: ≥ 50%)]. The following scoring system was used for PD-1: 0: < 1%, 1: ≥ 1–2%, 2: ≥ 2–5% and 3: > 5% of all TILs. For details of the different scores used see the Materials and Methods section. *NA* Not applicable. The legend above the visualization indicates the color code of the heatmap. **c** Exemplary immunohistochemical staining of CD8, MHC-I, PD-L1 and serial sections of PD-1 and LAG3



also given the small number of cases in total. Comparing PDS described as “CD8-high” with tumors showing lower levels of CD8-positive TILs, there was a tendency for a higher mean age and longer PFS of patients with “CD8-high” tumors, although not statistically significant due to the limited size of the cohort. The mean age of the three individuals with tumors described as “CD8-high” tumors was 86 ± 13.05 years versus 77.3 ± 10.7 years within the eight individuals where PDS tumors had been described as “CD8-low” ($p = 0.112$; Fisher’s exact test). For individuals with available clinical follow-up data, a mean PFS of 37.5 ± 13.05 months (two individuals described as “CD8-high”) versus 18 ± 13.5 months in five individuals with PDS tumors described as “CD8-low” could be observed.

CD3 showed similar results indicating that almost all infiltrating lymphocytes were CD8-positive TILs. In contrast, there were only very few CD20-positive B cells dispersed or in small clusters in a minority of cases.

RNA expression profiles

Performing NanoString analyses on 9 out of 14 PDS cases, the 3 PDS cases being defined as “CD8-high” were further analyzed using a multivariate differential analysis, revealing high levels of CD8-positive TILs (Fig. 1a, representative pictures 1c). Furthermore, a number of differentially expressed genes: *CD74*, *LYZ* and *HLA-B* were upregulated in “CD8-high”, whereas *CXCL14*, *HLA-A*, *IFI27*, *IFI6*, *IFITM1*, *S100A9*, *SPP1*, *TPM1* and *VCAN* were downregulated in “CD8-high” tumors compared to “CD8-low” tumors (see Fig. 2a). Moreover, one could observe elevated levels of immune-related cytokines such as *IL1A*, *IL2*, *IL4*, *IL6*, *IL10*, as well as various other pro-inflammatory immunomodulators (see Fig. 2b, genes flanking green bar), including *CD27*, and *CD40L*, both of which were very recently linked to enhanced response to CPI in malignant melanoma [28].

To further study the expression of known immune checkpoints/ligands, we specifically plotted the expression of these molecules (Fig. 2c). Interestingly, one case of “CD8-high” revealed high expression levels of multiple checkpoint/ligands, including *TIGIT*, *LAG-3*, *CTLA-4*, and *PDCD1* (encoding for PD-1), whereas the remaining ones showed a differential pattern of *CTLA-4*/*LAG-3* and *PDCD1* expression.

In addition, we detected several highly expressed genes in all nine PDS belonging to groups known as antigen-presenting machinery complex (*CD74*, *HLA-B*, *HLA-A*, *HLA-DR*, *HLA-DRB1*, *HLA-C*, *HLA-E*, and *HLA-DPA1*), cancer stem cell marker (*CD44*) and immune checkpoint/ligand group (*CD276*). Other highly expressed genes included *LYZ*, *RPL23*, *UBB*, *RPL7A*, *VCAN*, *IFI27*, *GLUL*, *TPH1*, *OAZ1*, *MFG8*, and *TPM1* (see Fig. S1).

Immunohistochemistry

MHC class I and II expression on tumor cells

To address changes in expression of molecules necessary for antigen presentation and effective immune response, we further analyzed the expression of MHC class I and MHC class II. Of 13 analyzable tumors, just 2 PDS demonstrated with a reduced expression of MHC class I showing scores of two, whereas all other 11 PDS showed a normal MHC-I expression with scores ≥ 5 . Four PDS revealed aberrant MHC class II expression on sarcoma cells ($> 5\%$ of tumor cells expressed MHC class II).

Interestingly, just 2 PDS tumors demonstrated a reduced expression of MHC class I showing scores of two, whereas all other 11 PDS showed a regularly high MHC-I expression with scores ≥ 5 .

Expression of immune-regulatory molecules (PD-1, PD-L1 and LAG-3) on tumor cells and tumor-infiltrating inflammatory cells

Five out of 14 PDS were completely PD-L1 negative (tumor as well as immune cells), while one case was scored as 5 ($\geq 50\%$ PD-L1-positive sarcoma cells, see Fig. 1c). This tumor, as well as eight additional PDS, were infiltrated by PD-L1-positive immune cells scored as 1 ($n = 4$) ($< 5\%$ PD-L1-positive immune cells), score 2 ($n = 1$) ($\geq 5 < 10\%$) and score 4 ($n = 4$) ($\geq 25 < 50\%$). LAG-3 was positive in seven tumors (score 1: $n = 2$; score 2: $n = 3$ and score 3: $n = 2$ cases) (see Fig. 1b). Eight out of 14 PDS tumors also revealed expression of PD-1 on immune cells (see Fig. 1b).

All three “CD8-high” PDS were infiltrated by PD-L1-positive immune cells (score 1 each) and LAG-3 (score 1 in one case and score 2 in two cases).

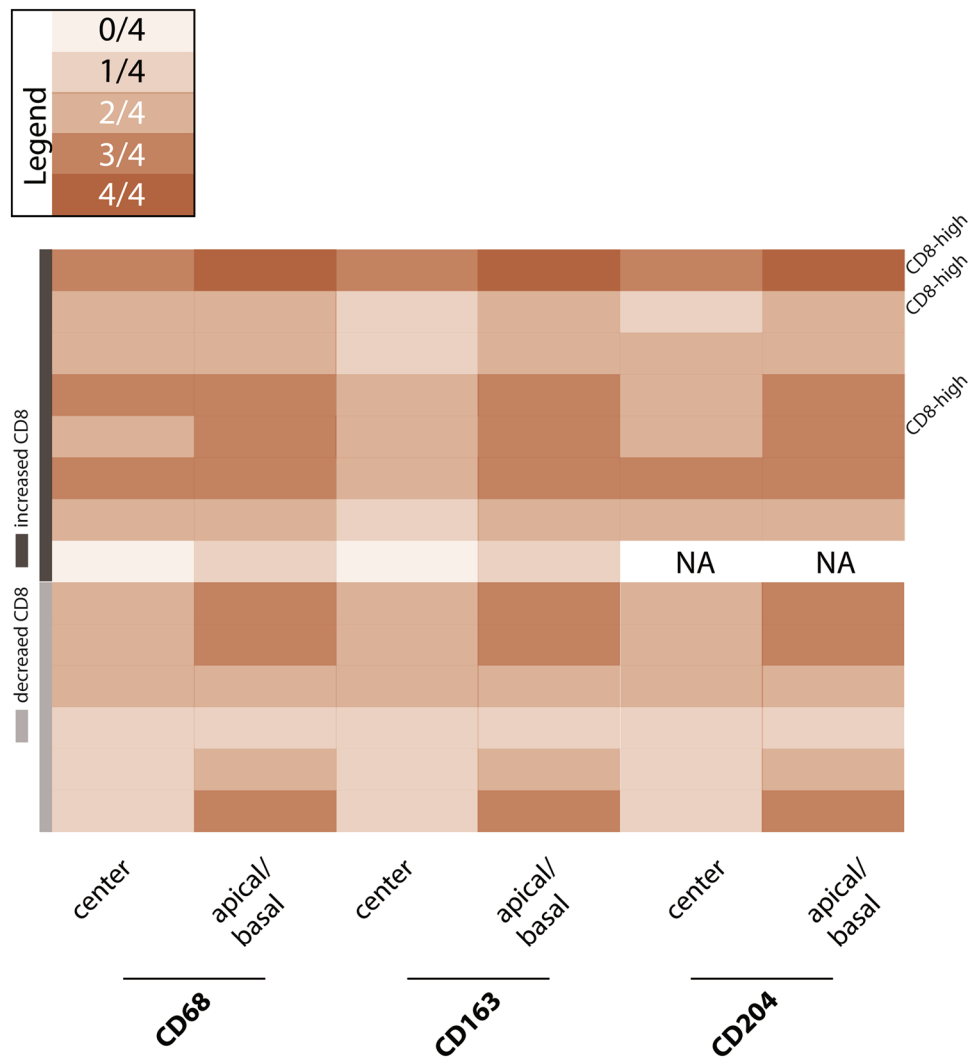
Tumor-associated macrophages

Tumor-associated macrophages (TAMs) predominantly consisted of CD68+ and CD163+CD204+M2 macrophages showing an accentuation at the invasion front in all PDS cases (see Fig. 3). There was no correlation between the amount of CD8-positive TILs and TAMs.

Discussion

As of now, the immune-environment of a given tumor appears to guide therapeutic decisions in cancer therapy. Our current study could work out that PDS tumors reveal an upregulation of genes being involved in immune responses, including molecules being involved in antigen presentation (Fig. 2, Fig. S1). In detail, the upregulated HLA class I

Fig. 3 Tumor-infiltrating macrophages. Tumor-infiltrating macrophages were graded semi-quantitatively using a grading system of five different categories, where “4” (also see legend) is representing high amounts of the indicated subtype of macrophages. The localization of the indicated population was further subdivided into central regions of the tumor, as well as apical/basal regions



immune-regulatory function of those genes in PDS. In detail, CXCL14 itself is a potent chemoattractant and activator for monocytes and dendritic cells, where it decreases the anti-tumor immune response [34]. Interestingly, our analyses revealed, that PDS show a M2-macrophages-rich microenvironment (without differences between “CD8-high” and “CD8-low” tumors) which may be a potential mechanism of PDS to avoid immune attack. In detail, M2 macrophages have a CD68 +, CD163 +, and CD204 + phenotype, inducing a local immunosuppression [35]. The tumor-promoting effects of M2 macrophages are further enhanced by secretion of matrix-degrading enzymes and angiogenic factors [36, 37].

Still, given that some cases revealed a low amount of CD8 TILs, one could find a rationale to explore the effect of a given therapeutic intervention previously linked to enhance infiltration of TILs in solid tumors. For instance, radiotherapy can enhance infiltration of tumors with TILs, and relieve a given myeloid-suppressive TME [38, 39].

The “CD8-high” PDS cases also showed elevated levels of *CD27* and *CD40L* that were very recently linked to response to immunotherapy in malignant melanoma [40]. In this context, an agonistic anti-CD27 treatment supported the maintenance of tumor-specific CD8 + T cells within the tumor and potentiated their ability to secrete IFN- γ upon coculture with tumor cells. In contrast, *CD40* ligand (*CD40L*), primarily expressed by activated CD4 + T cells, binds to CD40 on APCs, thereby inducing APC activation and in turn, priming of cytotoxic T lymphocytes [41, 42]. Moreover, two of three “CD8-high” PDS tumors showed strong MHC-I expression and all revealed infiltration by PD-L1-, PD-1- and LAG-3-expressing immune cells. Specifically, by looking at the expression pattern of multiple immune-checkpoints and ligands, one can conclude that there is a complex repertoire of different molecules being involved in the immune-evasion of PDS tumors. For instance, one case of “CD8-high” showed elevated levels of *HAVCR2/TIM-3*, as well as its ligand *LGALS9* (4th row,

Fig. 2c), while another case showed high levels of CTLA-4, as well as *PDCD1LG2* (third row, Fig. 2c).

Altogether, this implies that the majority of PDS, especially the “CD8-high” tumors, may induce an adequate anti-tumor immune response which could potentially be enhanced by targeting the described molecules on T cells, or by increasing the amount of CD8 cells in certain tumors in general. Only a minority of PDS seems to develop mechanisms to escape from being recognized by the immune cells through down-regulation of MHC class I molecules [43]. More specifically, the majority of cases was infiltrated by PD-L1-positive infiltrating immune cells ($n=9/13$), where 7 out of 13 tumors were infiltrated by LAG-3-expressing lymphocytes. Interestingly, 8 out of 14 PDS tumors also revealed expression of PD-1 on immune cells. In addition to PD-L1 expression, LAG-3 expression is a marker for activated immune response. Its inhibition enhanced the tumor cell-destroying inflammatory reaction in several tumor entities. Nevertheless, blocking of LAG-3 alone has shown modest effects, the anti-tumor efficacy can significantly be enhanced in combination with a PD-1 inhibitor [44]. The results of our RNA expression analysis, particularly the upregulation of HLA class I and II molecules, as well as an upregulation of the checkpoint molecules PD-L1 and LAG-3, let us hypothesize that patients with PDS could represent a cohort of patients that would benefit from CPI. Especially, “CD8-high” PDS with a high amount of tumor-infiltrating CD8-positive T cells seem to represent ideal candidates for this treatment option. Clinically, one should consider that PDS can also reveal low levels of CD8-positive TILs, and that interventions to increase the infiltration of these inflammatory cells in general need to be explored as a future direction for successful treatment with CPI. As shown in other tumor entities, a dual blockade of CTLA-4 and PD-1 or PD-1/PDL-1 and LAG-3 could probably enhance the efficacy of CPI monotherapies, also by rescuing CD8-positive T cells more vigorously from exhaustion than single signaling blockade [10, 45, 46].

Acknowledgements We thank Wiebke Jeske and Susann Zupp for technical assistance performing the TMA, mRNA in-situ and immunohistochemical staining.

Author contributions Sebastian Klein, Alexander Quaas and Doris Helbig designed the study, selected cases, conceived and carried out all experiments, analyzed and interpreted results, generated figures and tables, and performed literature research, and writing of the manuscript. Svenja Wagener-Ryczek and Maximilian Schoemmel were involved in performing the NanoString analyses. Cornelia Mauch and Reinhard Buettner were involved in designing the project. All the authors were involved in writing the paper and approved the final version of the manuscript.

Funding This work was supported by the Deutsche Forschungsgemeinschaft through the SFB829 (Z4 to Doris Helbig and Cornelia

Mauch) and the Else Kröner-Fresenius Stiftung (EKFS-2014-A06 and 2016_Kolleg.19 to Sebastian Klein).

Compliance with ethical standards

Conflict of interest The authors declare that they have no conflict of interest.

Ethical approval The study protocol conformed to the ethical guidelines of the 1975 Declaration of Helsinki as reflected by the approval of the institution’s human research review committee (Ethics Committee of the Medical Faculty of University of Cologne: registration no. 15–307).

Informed consent All patients gave written informed consent to the use of their tumors and their data for research.

Animal source Not applicable.

Cell line authentication Not applicable.

References

1. Tardio JC, Pinedo F, Aramburu JA, Suarez-Massa D, Pampin A, Requena L, Santonja C (2016) Pleomorphic dermal sarcoma: a more aggressive neoplasm than previously estimated. *J Cutan Pathol* 43:101–112. <https://doi.org/10.1111/cup.12603>
2. Miller K, Goodlad JR, Brenn T (2012) Pleomorphic dermal sarcoma: adverse histologic features predict aggressive behavior and allow distinction from atypical fibroxanthoma. *Am J Surg Pathol* 36:1317–1326. <https://doi.org/10.1097/PAS.0b013e31825359e1>
3. Helbig D, Ihle MA, Putz K, Tantcheva-Poor I, Mauch C, Buttner R, Quaas A (2016) Oncogene and therapeutic target analyses in a typical fibroxanthomas and pleomorphic dermal sarcomas. *Oncotarget* 7(16), 21763–21774. <https://doi.org/10.18632/oncotarget.7845>
4. Helbig D, Quaas A, Mauch C et al (2017) Copy number variations in atypical fibroxanthomas and pleomorphic dermal sarcomas. *Oncotarget* 8:109457–109467. <https://doi.org/10.18632/oncotarget.22691>
5. Brahmer JR, Tykodi SS, Chow LQ et al (2012) Safety and activity of anti-PD-L1 antibody in patients with advanced cancer. *N Engl J Med* 366:2455–2465. <https://doi.org/10.1056/NEJMoa1200694>
6. Yarchoan M, Hopkins A, Jaffee EM (2017) Tumor Mutational burden and response rate to PD-1 inhibition. *N Engl J Med* 377:2500–2501. <https://doi.org/10.1056/NEJMc1713444>
7. Borradori L, Sutton B, Shayesteh P, Daniels GA (2016) Rescue therapy with anti-programmed cell death protein 1 inhibitors (PD-1) of advanced cutaneous squamous cell carcinoma and basosquamous carcinoma: preliminary experience in 5 cases. *Br J Dermatol* 175(6):1382–1386 <https://doi.org/10.1111/bjd.14642>
8. McGranahan N, Furness AJ, Rosenthal R et al (2016) Clonal neoantigens elicit T cell immunoreactivity and sensitivity to immune checkpoint blockade. *Science* 351:1463–1469. <https://doi.org/10.1126/science.aaf1490>
9. Mo Z, Liu J, Zhang Q et al (2016) Expression of PD-1, PD-L1 and PD-L2 is associated with differentiation status and histological type of endometrial cancer. *Oncol Lett* 12:944–950. <https://doi.org/10.3892/ol.2016.4744>
10. Nghiem PT, Bhatia S, Lipsen EJ et al (2016) PD-1 Blockade with pembrolizumab in advanced merkel-cell carcinoma. *N Engl J Med* 374:2542–2552. <https://doi.org/10.1056/NEJMoa1603702>

11. Valkenburg KC, de Groot AE, Pienta KJ (2018) Targeting the tumour stroma to improve cancer therapy. *Nat Rev Clin Oncol* 15:366–381. <https://doi.org/10.1038/s41571-018-0007-1>
12. Barberis I, Martini M, Iavarone F, Orsi A (2016) Available influenza vaccines: immunization strategies, history and new tools for fighting the disease. *J Prev Med Hyg* 57:E41–E46
13. Afanasiev OK, Yelistratova L, Miller N, Nagase K, Paulson K, Iyer JG, Ibrani D, Koelle DM, Nghiem P (2013) Merkel polyomavirus-specific T cells fluctuate with merkel cell carcinoma burden and express therapeutically targetable PD-1 and Tim-3 exhaustion markers. *Clin Cancer Res* 19:5351–5360. <https://doi.org/10.1158/1078-0432.CCR-13-0035>
14. Ohaegbulam KC, Assal A, Lazar-Molnar E, Yao Y, Zang X (2015) Human cancer immunotherapy with antibodies to the PD-1 and PD-L1 pathway. *Trends Mol Med* 21:24–33. <https://doi.org/10.1016/j.molmed.2014.10.009>
15. Herbst RS, Soria JC, Kowanetz M et al (2014) Predictive correlates of response to the anti-PD-L1 antibody MPDL3280A in cancer patients. *Nature* 515:563–567. <https://doi.org/10.1038/nature14011>
16. Chapuis AG, Ragnarsson GB, Nguyen HN et al. (2013) Transferred WT1-reactive CD8+ T cells can mediate antileukemic activity and persist in post-transplant patients. *Sci Transl Med* 5:174ra27. <https://doi.org/10.1126/scitranslmed.3004916>
17. Leone P, Shin EC, Perosa F, Vacca A, Dammacco F, Racanelli V (2013) MHC class I antigen processing and presenting machinery: organization, function, and defects in tumor cells. *J Natl Cancer Inst* 105:1172–1187. <https://doi.org/10.1093/jnci/djt184>
18. Adams JL, Smothers J, Srinivasan R, Hoos A (2015) Big opportunities for small molecules in immuno-oncology. *Nat Rev Drug Discov* 14:603–622. <https://doi.org/10.1038/nrd4596>
19. Tran E, Robbins PF, Lu YC et al (2016) T-cell transfer therapy targeting mutant KRAS in cancer. *N Engl J Med* 375:2255–2262. <https://doi.org/10.1056/NEJMoa1609279>
20. McCalmont TH (2012) Correction and clarification regarding AFX and pleomorphic dermal sarcoma. *J Cutan Pathol* 39:8. <https://doi.org/10.1111/j.1600-0560.2011.01851.x>
21. Bankhead P, Loughrey MB, Fernandez JA et al (2017) QuPath: open source software for digital pathology image analysis. *Sci Rep* 7:16878. <https://doi.org/10.1038/s41598-017-17204-5>
22. Allred DC, Harvey JM, Berardo M, Clark GM (1998) Prognostic and predictive factors in breast cancer by immunohistochemical analysis. *Mod Pathol* 11:155–168
23. Johnson DB, Estrada MV, Salgado R et al (2016) Melanoma-specific MHC-II expression represents a tumour-autonomous phenotype and predicts response to anti-PD-1/PD-L1 therapy. *Nat Commun* 7:10582. <https://doi.org/10.1038/ncomms10582>
24. Scheel AH, Dietel M, Heukamp LC et al (2016) Harmonized PD-L1 immunohistochemistry for pulmonary squamous-cell and adenocarcinomas. *Mod Pathol* 29:1165–1172. <https://doi.org/10.1038/modpathol.2016.117>
25. Herbst RS, Baas P, Kim DW et al (2016) Pembrolizumab versus docetaxel for previously treated, PD-L1-positive, advanced non-small-cell lung cancer (KEYNOTE-010): a randomised controlled trial. *Lancet* 387:1540–1550. [https://doi.org/10.1016/S0140-6736\(15\)01281-7](https://doi.org/10.1016/S0140-6736(15)01281-7)
26. Fehrenbacher L, Spira A, Ballinger M et al (2016) Atezolizumab versus docetaxel for patients with previously treated non-small-cell lung cancer (POPLAR): a multicentre, open-label, phase 2 randomised controlled trial. *Lancet* 387:1837–1846. [https://doi.org/10.1016/S0140-6736\(16\)00587-0](https://doi.org/10.1016/S0140-6736(16)00587-0)
27. Jensen TO, Schmidt H, Moller HJ, Hoyer M, Maniecki MB, Sjoegren P, Christensen IJ, Steiniche T (2009) Macrophage markers in serum and tumor have prognostic impact in American joint committee on cancer stage I/II melanoma. *J Clin Oncol* 27:3330–3337. <https://doi.org/10.1200/JCO.2008.19.9919>
28. Auslander N, Zhang G, Lee JS et al (2018) Robust prediction of response to immune checkpoint blockade therapy in metastatic melanoma. *Nat Med* 24:1545–1549. <https://doi.org/10.1038/s41591-018-0157-9>
29. Chowell D, Krishna S, Becker PD et al (2015) TCR contact residue hydrophobicity is a hallmark of immunogenic CD8+ T cell epitopes. *Proc Natl Acad Sci USA* 112:E1754–E1762. <https://doi.org/10.1073/pnas.1500973112>
30. Rizvi NA, Hellmann MD, Snyder A et al (2015) Cancer immunology. Mutational landscape determines sensitivity to PD-1 blockade in non-small cell lung cancer. *Science* 348:124–128. <https://doi.org/10.1126/science.aaa1348>
31. Snyder A, Makarov V, Merghoub T et al (2014) Genetic basis for clinical response to CTLA-4 blockade in melanoma. *N Engl J Med* 371:2189–2199. <https://doi.org/10.1056/NEJMoa1406498>
32. Van Allen EM, Miao D, Schilling B et al (2015) Genomic correlates of response to CTLA-4 blockade in metastatic melanoma. *Science* 350:207–211. <https://doi.org/10.1126/science.aad0095>
33. Qian J, Luo F, Yang J et al (2018) TLR2 Promotes glioma immune evasion by downregulating MHC class II molecules in microglia. *Cancer Immunol Res* 6:1220–1233. <https://doi.org/10.1158/2326-6066.CIR-18-0020>
34. Starnes T, Rasila KK, Robertson MJ, Brahmi Z, Dahl R, Christopherson K, Hromas R (2006) The chemokine CXCL14 (BRAK) stimulates activated NK cell migration: implications for the downregulation of CXCL14 in malignancy. *Exp Hematol* 34:1101–1105. <https://doi.org/10.1016/j.exphem.2006.05.015>
35. Kudjawi YC, Chatellier G, Decool E, de Maria F, Beltzer N, Gremy I, Meyer G, Eilstein D (2016) Timing in initiating lung cancer treatment after bronchoscopy in France: study from medico-administrative database. *Lung Cancer* 95:44–50. <https://doi.org/10.1016/j.lungcan.2016.02.016>
36. Mantovani A, Sica A, Locati M (2007) New vistas on macrophage differentiation and activation. *Eur J Immunol* 37:14–16. <https://doi.org/10.1002/eji.200636910>
37. Falleni M, Savi F, Tosi D, Agape E, Cerri A, Moneghini L, Bulfamante GP (2017) M1 and M2 macrophages' clinicopathological significance in cutaneous melanoma. *Melanoma Res* 27:200–210. <https://doi.org/10.1097/CMR.0000000000000352>
38. Rodriguez-Ruiz ME, Rodriguez I, Garasa S et al (2016) Abscopal effects of radiotherapy are enhanced by combined immunostimulatory mAbs and are dependent on CD8 T cells and crosspriming. *Cancer Res* 76:5994–6005. <https://doi.org/10.1158/0008-5472.CAN-16-0549>
39. Wu Q, Allouch A, Martins I, Modjtahedi N, Deutsch E, Perfettini JL (2017) Macrophage biology plays a central role during ionizing radiation-elicited tumor response. *Biomed J* 40:200–211. <https://doi.org/10.1016/j.bj.2017.06.003>
40. Wasiuk A, Testa J, Weidlick J et al (2017) CD27-Mediated regulatory T cell depletion and effector T cell costimulation both contribute to antitumor efficacy. *J Immunol* 199:4110–4123. <https://doi.org/10.4049/jimmunol.1700606>
41. Roberts DJ, Franklin NA, Kingeter LM, Yagita H, Tutt AL, Glennie MJ, Bullock TN (2010) Control of established melanoma by CD27 stimulation is associated with enhanced effector function and persistence, and reduced PD-1 expression of tumor infiltrating CD8(+) T cells. *J Immunother* 33:769–779. <https://doi.org/10.1097/CJI.0b013e3181ee238f>
42. Soong RS, Song L, Trieu J, Lee SY, He L, Tsai YC, Wu TC, Hung CF (2014) Direct T cell activation via CD40 ligand generates high avidity CD8+ T cells capable of breaking immunological tolerance for the control of tumors. *PLoS One* 9:e93162. <https://doi.org/10.1371/journal.pone.0093162>
43. van Houdt IS, Oudejans JJ, van den Eertwegh AJ et al (2005) Expression of the apoptosis inhibitor protease inhibitor 9 predicts clinical outcome in vaccinated patients with stage III and

- IV melanoma. *Clin Cancer Res* 11:6400–6407. <https://doi.org/10.1158/1078-0432.CCR-05-0306>
44. Woo SR, Turnis ME, Goldberg MV et al (2012) Immune inhibitory molecules LAG-3 and PD-1 synergistically regulate T-cell function to promote tumoral immune escape. *Cancer Res* 72:917–927. <https://doi.org/10.1158/0008-5472.CAN-11-1620>
45. Kaufman HL, Russell J, Hamid O et al (2016) Avelumab in patients with chemotherapy-refractory metastatic Merkel cell carcinoma: a multicentre, single-group, open-label, phase 2 trial. *Lancet Oncol* 17:1374–1385. [https://doi.org/10.1016/S1470-2045\(16\)30364-3](https://doi.org/10.1016/S1470-2045(16)30364-3)
46. Brahmer J, Reckamp KL, Baas P et al (2015) Nivolumab versus docetaxel in advanced squamous-cell non-small-cell lung cancer. *N Engl J Med* 373:123–135. <https://doi.org/10.1056/NEJMoa1504627>

Publisher's Note Springer Nature remains neutral with regard to jurisdictional claims in published maps and institutional affiliations.